SpaceOps Conferences
28 May - 1 June 2018, Marseille, France
2018 SpaceOps Conference

10.2514/6.2018-2537

Flight Dynamics Operational Experience from ExoMars TGO aerobraking campaign at Mars

F. Castellini[1]
Telespazio-VEGA Deutschland (located at ESA/ESOC), Darmstadt, Hessen, 64293, Germany, Francesco.Castellini@esa.int

G. Bellei[1]
Deimos Space (located at ESA/ESOC), Darmstadt, Hessen, 64293, Germany, Gabriele.Bellei@esa.int

and
B. Godard[1]
Telespazio-VEGA Deutschland (located at ESA/ESOC), Darmstadt, Hessen, 64293, Germany, Bernard.Godard@esa.int

This paper aims at giving a Flight Dynamics perspective on ExoMars Trace Gas Orbiter aerobraking operations, discussing the main challenges for both navigation and spacecraft commanding, describing the work-flow of activities within an operations cycle and presenting some results from the successful campaign, together with the most important lessons learnt.

I. Introduction

ESA's ExoMars Trace Gas Orbiter (TGO) was launched by a Roscosmos provided Proton-M launcher from Baikonur on March 14th 2016, carrying the Schiaparelli Entry, descent and landing Demonstrator Module (EDM). Together, TGO and EDM constitute the first mission of the ExoMars Programme, a cooperation between the European Space Agency (ESA), Roscosmos and NASA which also includes a 2020 mission composed of a Carrier Module (CM) and a Descent Module (DM) delivering a Rover and a Surface science Platform (RSP). See for example Ref. [1] for high level overview on the 2016 mission, and Ref. [2] for a more detailed description of the overall ExoMars Programme mission analysis.

The TGO-EDM Spacecraft (S/C) composite was inserted by Proton-M into a direct injection Type-II transfer to Mars, reaching the Red Planet after a 7-month cruise phase including two large Deep Space Manoeuvres (DSM). After releasing the EDM on the planned trajectory for Mars landing on October 16th, TGO successfully performed its Mars Orbit Insertion (MOI) on October 19th, entering a 4-sol, equatorial, highly elliptical orbit. Through a series of chemical manoeuvres, this was changed in early 2017 into a 1-sol, 74 degrees inclination orbit. From here, TGO started aerobraking operations on March 14th 2017, intended to gradually reduce the orbital period from ~24 hours down to ~2 hours with limited use of propellant. After an extremely intense and challenging year of aerobraking operations, interrupted only by a solar conjunction wait-out period in July and August, TGO successfully completed its aerobraking phase on February 20th 2018, after having reached the target apocentre altitude of ~1000 km. Thereafter, a 6-week chemical manoeuvre campaign brought TGO to the final science orbit, a 360x413 km "frozen" orbit for which eccentricity and argument of pericentre are approximately constant, with a 373:30 resonance with Mars rotational period. Since mid-April 2018, TGO has started its science and relay missions, studying Mars with four remote sensing payloads and ready to act as communications relay for existing and future NASA/ESA surface assets.

An extensive overview of TGO aerobraking design, preparations and operations, covering all involved parties (Industrial consortium developing the S/C, all teams at the Mission Control Centre at ESOC, Project at ESTEC), is given in Ref. [3]. The present paper is instead aimed at giving a Flight Dynamics (FD) point of view, with particular focus on the challenges presented by the TGO design and setup of its on-board autonomy features, by the unpredictability of the Martian atmosphere and by the large FD workload necessary to satisfy stringent ground prediction requirements, resulting in very frequent ground navigation cycles. Although some details will be provided on specific aspects of the involved FD disciplines, the focus of the paper is on system level FD operations, trying to identify, describe and quantitatively assess those aspects that drove the performances of TGO aerobraking, as well as the overall FD effort and key decisions.

[1] Flight Dynamics Engineer, Science Missions FD Support Section, ESOC.

The continuation of the paper is split in three main sections. In the first, the challenges faced by the FD team in relation to aerobraking at Mars and TGO characteristics are addressed, also highlighting some specific design features that would, in retrospect, have allowed easier operability. The second section describes the "FD cycles" regularly carried out during aerobraking to reconstruct and plan the S/C trajectory as well as to produce Guidance, Navigation and Control (GNC) commands for the S/C. The third discusses the main results from almost one year of successful FD aerobraking operations, in terms of both the performance of the S/C and of the ground team. Finally, the main lessons learnt are summarized in the conclusion, together with some suggestions for future aerobraking missions, always with a focus on the FD aspects.

The design of TGO's GNC hardware and functionalities, complex Failure Detection Isolation and Recovery (FDIR) and on-board autonomy functions, will only be addressed in this paper for specific parts which have direct relevance with the FD topics under examination. The same approach is taken for the description of all analysis, testing, integration and other activities carried out by the large ESA/Industry team in preparation of the aerobraking, as well as for the high level strategy, planning and execution of operations by the above entities. A broad but complete overview of these topics is given in Ref. [3], which this paper complements by providing a FD perspective. A preview of the aerobraking strategy as conceived in 2012 is presented instead in Ref. [4], while Ref. [5] and [6] provide additional information on TGO design and on its initial operations: launch and near-Earth commissioning, cruise, DSMs, EDM targeting and EDL, TGO MOI and post-MOI manoeuvres campaign.

II.TGO Aerobraking Challenges for Flight Dynamics

Aerobraking is a technique by which a S/C can reduce its orbital energy through aerodynamic drag, by passing through the upper layers of a planet's atmosphere at each pericentre, and therefore allowing to save large quantities of propellant when targeting near-circular low orbits from initial highly elliptical orbits. For a typical low Mars orbit mission, this ensures savings in the order of 1 km/s of ΔV. Aerobraking was pioneered in 1993 at NASA JPL for the Magellan mission around Venus [7], and has since then been used by JPL around Mars for several missions: Mars Global Surveyor (MGS) between September 1997 and February 1999 (from 47.5 to 2.0 hours orbital period, [8,9]), Mars Odyssey (ODY) between November 2001 and February 2002 (from 18.6 to 1.9 hour, [10,11]), and Mars Reconnaissance Orbiter (MRO) from March to August 2006 (from 35.5h to 1.9 hour, [12,13]). On the basis of the success of these experiences, ESA decided to employ aerobraking to reach TGO's target low Mars orbit, with the technical support of the JPL navigation team. Previously, ESA's only relevant experience was a test aerobraking campaign for the Venus Express (VEX) S/C [14], carried out as a high risk activity just before reaching end of life in 2014. VEX only had rudimental aerobraking capabilities, with a dedicated aero-pass mode but no autonomy or safety features, but it provided ESOC's FD team with hands-on experience in navigating and commanding a S/C through the atmosphere, which would become valuable for TGO, designed for operational aerobraking.

Although TGO's aerobraking was a success, safely bringing the S/C to its target science and relay orbit in less than a year and with large propellant savings, it presented serious challenges to the FD team at ESOC, which invested large resources in both the preparation phase and the actual flight operations. First of all, aerobraking around Mars is inherently risky, requiring accurate navigation in spite of unpredictable atmospheric density, a robust S/C with autonomous functions to deal with both nominal timeline and contingencies, an equally robust operational approach with sufficient safety margins, and a large team to cope with a critical operations phase involving daily navigation and possibly commanding activities. Moreover, although TGO was designed as an aerobraking mission, some of its physical characteristics and on-board features were driven by other factors, as its role as EDM carrier and the partial reuse of an existing S/C platform, hence making it not ideal for this operation. Even after EDM separation and with most of the propellant used for cruise, MOI and Mars orbital changes, TGO is in fact a large, not very agile, S/C. During aerobraking, TGO had a mass of around 1750 kg, inertias of ~(4500, 5800, 2500) kg·m^2, Solar Arrays (SA) of 22 m^2 and a total exposed area during aerodynamic passes of 29 m^2, relying on 4 relatively small 25 Nms Reaction Wheels (RW) for slews, due to a rather inefficient force-free thruster configuration resulting in 2.5x consumption with respect to the unbalanced mode. The direct consequences of these characteristics are long slew times, up to 54 minutes for a worst-case 180 deg rotation around the least agile Y axis, and a very large ballistic coefficient of ~60 kg/m^2. Moreover, thermal and mechanical constraints with the chosen Multi-Layer Insulation (MLI) and SA wings defined survivability limits of 2800 W/m^2, 500 kJ/m^2 and 700 mPa. For comparison, NASA's MGS/ODY/MRO respectively had ballistic coefficients during aerobraking of roughly 42/42/35 kg/m^2 for approximate masses of 760/460/1300 kg, and were designed with MLI withstanding heat fluxes in the order of 5000 W/m^2. From these numbers, it's clear how the first major challenge was the length of TGO's aerobraking from the initial 24 hour orbit, with about 10 months of active drag passes imposing a large workload, particularly on FD but also on Flight Control Team (FCT) and other supporting teams, due to the much lower achievable ΔV per pass with respect to other S/C. For instance, the average

and largest ΔV per pass for TGO were ~1.1 m/s and ~2.7 m/s, against ~6.0 m/s and ~2.7 m/s for MRO [13]. While MGS also required a long aerobraking phase due to launch damage to a solar array, forcing a drastic reduction in the allowed dynamic pressures and a complete mission re-planning, ODY and MRO reached their final orbits in only 3 and 5 months from initial orbits of 18 and 35 hour orbital periods.

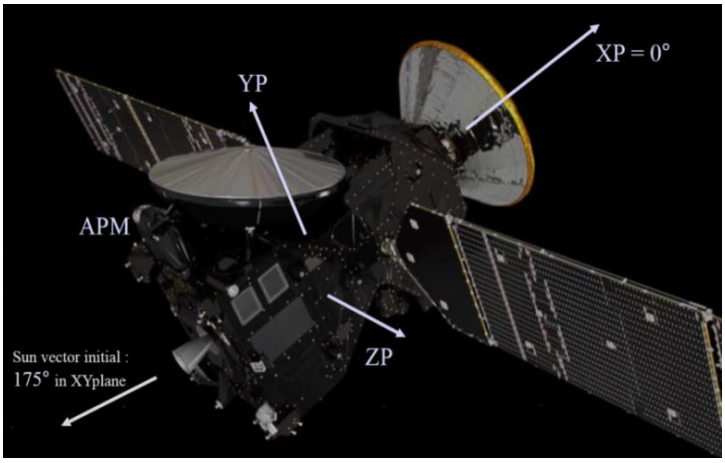

Figure 1: TGO external layout and reference frame

Mass	1750 kg
Inertias	(4500, 5800, 2500) kg m^2
SA area	22.0 m^2
Total front area	29.3 m^2
Ballistic Coefficient	60 kg/m^2
Heat Flux Limit	2800 W/m^2
Heat Load Limit	500 kJ/m^2
Dyn. Pressure Limit	700 mPa
10-Newton RCTs (Reaction Control Thrusters)	4x2 pitch/yaw 4x2 roll (balanced) 2x2 force-free
RW	4x 25 Nms (tetrahedral)
Worst-case slew	54 minutes

Table 1: Main TGO characteristics in its aerobraking configuration

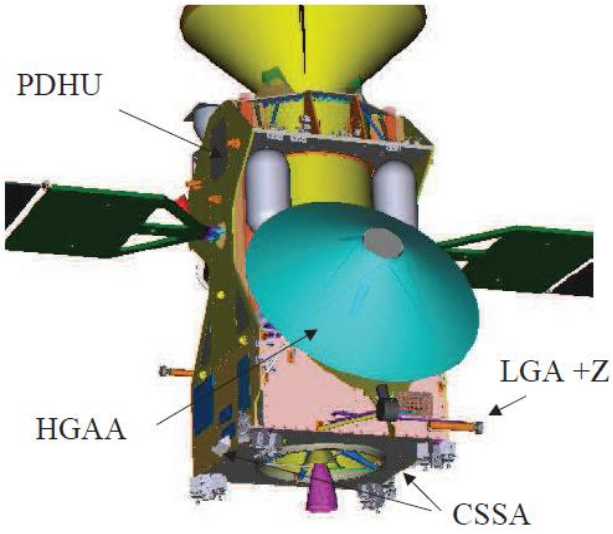

Figure 2 a): TGO front view, from +Y

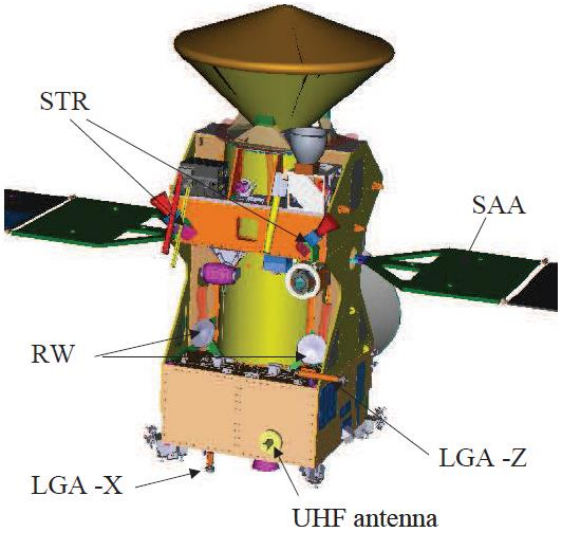

Figure 2 b): TGO rear view, from –Y

The second major challenge for the FD team was to devise an operational strategy that would allow to fit all S/C activities within the orbit for the lowest foreseen orbital periods of ~2 hours in the so called "end-game" phase, subject to agility constraints imposed by the TGO design. For any aerobraking S/C, three different attitudes need to be flown in different parts of an orbit: an aerodynamically stable atmospheric attitude close to pericentre, aimed at maximizing the frontal area and hence the drag acceleration, a quasi-inertial exoatmospheric attitude allowing to point the High Gain Antenna (HGA) to Earth for communications, and an Orbit Control Manoeuvre (OCM) attitude for those apocentre when a pericentre lowering or raising burn is needed for aerobraking corridor control. For TGO, the resulting sequence of activities for an orbit with OCM is shown in Figure 3. Safe aero-pass configuration is achieved through a dedicated GNC thruster controlled Aerobraking Mode (AEBM), with large control dead-bands designed to avoid pitch/yaw actuations thanks to aerodynamic stability, which is achieved with the air-flow mostly on –X axis, slightly canted towards +Y by about 10 deg [3]. Due to the large control errors when exiting AEBM (up to 50 deg per axis), a continuous guidance profile could not be commanded from ground, with TGO relying on its Large Angle Proportional Integral Derivative (LAPID) controller to autonomously slew, on RWs, to Earth communications attitude. Guided RW slews could instead be used when going from exoatmospheric to OCM and back to atmospheric attitudes, with a Wheel Off-Loading (WOL) executed at each orbit to unload the wheels from the effect of disturbance torques, mainly gravity gradient. Note that LAPID slews with TGO's implementation are rate limited, resulting in significantly longer

slew times with respect to guided slews, up to 54 minutes. By comparison, MRO was able to perform RW slews in less than 10 minutes. Table 2 summarizes the worst-case duration of each activity when using the original operational strategy, which included a constraint to keep the HGA fixed in stowed position throughout the entire aerobraking, due to safety concerns for possible issues with the Antenna Pointing Mechanism (APM), potentially resulting in a risky atmospheric pass with deployed HGA. This strategy was followed in the first months of aerobraking before solar conjunction, with an orbital period decreasing from 24 to ~14 hours, therefore still with large time margins in the orbit, but could not be afforded until the end-game phase with orbital periods close to 2 hours.

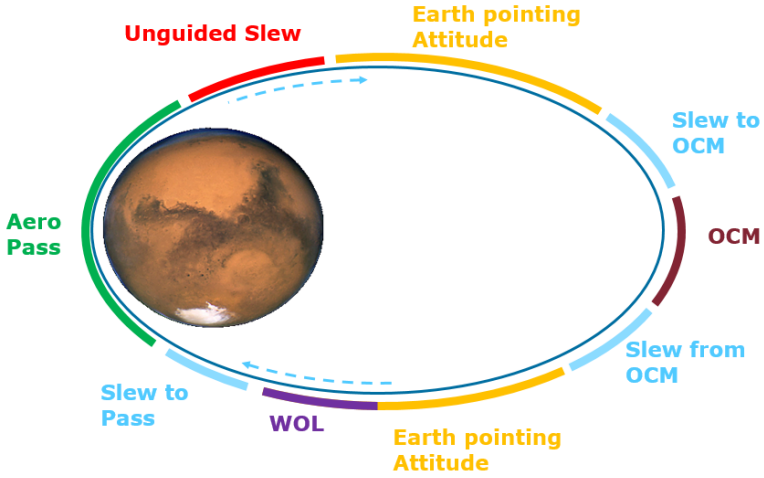

Figure 3:Nominal activities in aerobraking orbit with OCM

Activity	Worst-case duration
Aero-pass	31 min: 15 min drag + 8 min margin + 4 min rate damping
Unguided slew	54 min
Slew to OCM	30 min
OCM	5 min
Slew from OCM	30 min
WOL	15 min
Slew to Aero-pass	30 min
Total with OCM	3 hour 15 min
Total without OCM	2 hour 10 min
Target orbit period	~2 hours

Table 2:Timeline of activities in nominal aerobraking orbit with OCM (fixed HGA)

Although feasible even in the end-game for specific orbital geometries, the original strategy with fixed HGA was not robust to worst-case geometries, required very expensive force-free RCT slews to perform OCMs in short orbits (~300 grams of propellant per slew), and did not allow for sufficient margins in terms of neither mean SA power nor communication windows for Telemetry (TM) dumps, Telecommand (TC) uplinks and tracking data collection. After extensive FD analyses and several iterations with the FCT and the industrial support team, it was therefore decided to remove the constraint on the HGA outside of the aero-passes, i.e. moving the APM at AEBM exit to point to the Earth as soon as possible, therefore greatly reducing the required slew duration. Figure 4 and 5 show the average Sun flux and the communications duration in an orbit without OCMs as a function of the orbital period for different strategies. Moving the HGA allowed to reach the minimum 300 W/m^2 required to operate TGO and to keep ~30 minutes (plus 2-Way Light-Time) of TC uplink capability even for the shortest orbits. Moreover, it also allowed to avoid expensive RCT slews in short orbits with Pericentre Raising Manoeuvres (PRMs), for which the attitude is similar to the aero-pass one, whereas Pericentre Lowering Manoeuvres (PLMs) would still have to be performed on thrusters for the last 2 weeks of aerobraking. After thorough FD testing, Industry approval and further validation by the FCT on both the operational simulator (SIM) and TGO's Avionics Test bench (ATB), the new strategy was phased into flight operations after solar conjunction, in September 2017. The final apocentre altitude was reached several months later, after successfully flying the end-game short orbits, with the added bonus of never having relied on thrusters for slewing, since PLMs turned out not to be necessary in the last two weeks of operations. See Ref. [3] for a comprehensive overview at system level of the preparations, validation, timeline and execution of operations.

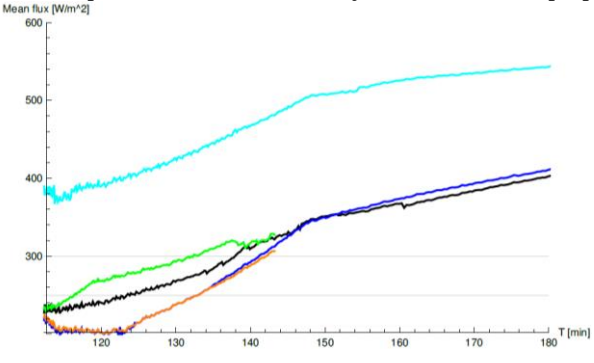

Figure 4:Mean Sun flux over an entire orbit with different commanding strategies

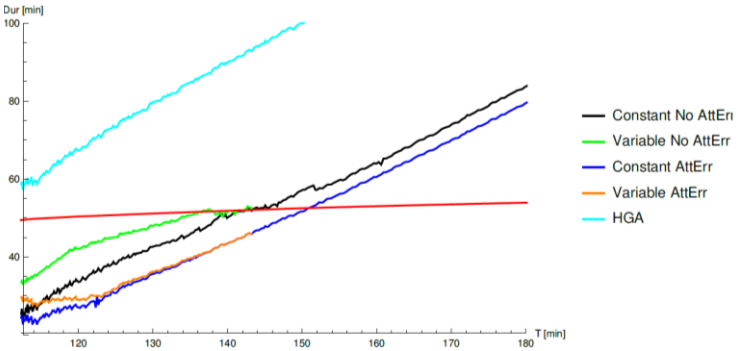

Figure 5:Mean communication window for orbits without OCM) with different commanding strategies

Another significant obstacle which had to be overcome by the operations teams was the complex set-up and trouble-shooting of TGO's on-board functions. The GNC software incorporates in fact a high level of autonomy supporting aerobraking, as well as a dedicated FDIR structure aiming at protecting the S/C in case of contingencies. In particular: 1) an accelerometer based Pericentre Time Estimator (PTE) was used to nominally shift the on-board Mission Timeline (MTL) after each aero-pass, in order to drastically reduce the time spent in AEBM by removing most of the margins needed to account for pericentre time ground prediction errors; 2) autonomous PRMs could be triggered by different FDIRs to either tune the aerobraking corridor in case of exceeded thermal constraints (Flux Reduction Manoeuvres, FRM) or to completely get out of the atmosphere in case of a more serious anomaly leading to safe mode (Safe Pop-up Manoeuvres, SPM); 3) an Atmosphere Detector (ATMD) estimated the external torques from the gyro measurements and triggered entry in an Atmospheric Rate Damping (ARD) sub-mode of the thruster controlled GNC modes after a safe mode, in order to ensure survivability to aero-passes in non-aerodynamically stable attitudes; and 4) a Pop-Up Direction Estimator (PUDE) function was even implemented to allow for a SPM in the unlikely case of both Star Trackers (STR) being unable to acquire an attitude, e.g. due to solar flare conditions or any other anomaly. While critical for a successful aerobraking, such autonomies – for which more information can be found in Ref. [3] - were extremely complex to set-up in the preparatory phase, as well as to troubleshoot in the first weeks of operations and to continuously re-tune when needed during aerobraking. Together with the design and updating of the aerodynamic corridor and Long Term Planning (LTP) trajectory [3], this required a large FD effort in support of the FCT, as well as deep industrial involvement in the definition or modification, and validation, of Flight Operational Procedures (FOP), S/C Parameter/Functional Monitoring (PMONs/FMONs) for FDIR purposes, Actions Sequences (ACSEQ), Delayed TC Files (DTCFs) and On-Board Control Procedures (OBCPs) for autonomous, conditional execution of command sequences, and On-Board Software (OBSW) updates to fix specific issues or improve the S/C operability.

A complete list of these updates, carried out over a period of more than 2 years from the first ATB tests until end of operations, is out of the scope of this paper. As an example of S/C trouble-shooting, several cases of interference between nominal and aerobraking FDIRs and functions were discovered when first testing AEBM in flight during the walk-in of March 2017. For instance, it was found that local reconfigurations (e.g. SA drive electronics due to resistance sensor issues or STR due to internal health check) during AEBM would affect PTE predictions, or that PUDE measurements would be forgotten in the case of a STR swap. These issues were fixed in flight, first with operational work-around and then with a complete OBSW update – covering also other aspects - during solar conjunction, resulting in an initial delay which was however recovered with a slightly more aggressive aerobraking regime. As for examples of in-flight tuning of parameters, the PMON limit on the peak pass acceleration for the triggering of FRMs was updated several times throughout the aerobraking [3], similarly the PUDE thresholds for minimum instantaneous acceleration was reduced to improve the likelihood of successful pop-up direction detection, and the aerodynamic stability angle defining the reference attitude in the S/C XY plane was modified by about 4 deg to reduce the maximum rates and hence propellant consumption during aero-passes. Examples of new OBCPs/DTCFs include those for assisted STR acquisition, i.e. feeding the attitude information from the Gyro-Stellar Estimation for direct initialization of the tracking mode without going through the "lost-in-space" acquisition after a blinding) and for manual execution of SPM. This last activity was particularly interesting on FD side, foreseeing ground attitude determination in case of a safe mode followed by both STRs being unable to acquire and PUDE either disabled or unable to estimate the pop-up direction due to too low acceleration, an unlikely but not impossible scenario for the risky end-game. In such a case, ground would manually command the pop-up, using attitude information reconstructed from the Doppler signature given by TGO's spinning motion around Sun direction, then waiting for STR acquisition and safe mode recovery safely out of the atmosphere. This scenario luckily never materialized, but preparations were extremely demanding, involving all FD subsystems, FCT and Industry.

Another important task which completes the list of the main aerobraking challenges faced by the FD team, was the daily monitoring of both the Martian atmosphere and the behaviour of all GNC units and functions. In particular, two possible limiting factors were identified, which could lead to the failure of the operational concept and possibly put the safety of the S/C at risk, especially in the critical end-game. First, as described above, the S/C schedule in short orbits was extremely tight. This included, upon Industry recommendation, 8 minutes of margin (4 before and 4 after each pass) for the prediction errors of the PTE function. That is, TGO was commanded to AEBM mode 4 min before reaching a predicted dynamic pressure of 0.5 mPa, and then from Pass to Rate Damping (RD) sub-mode 4 min after dropping below such value again. The OBSW would then shift all Mission Timeline (MTL) commands after each pericentre based on the difference between the PTE on-board prediction using information from the last two passes [3] and the ground commanded table of pericentre times. If the PTE prediction error was however larger than the 4 minute margin, the S/C may have entered AEBM too late or exited it too early, probably triggering a safe mode in NOMR (Nominal Mode with RW) due to the wheels being unable to cope with the aerodynamic torques. While the

PTE was expected to predict the next pericentre time with errors typically lower than 4 min, it was also known that its accuracy would start degrading due to the increasing asymmetry of acceleration profiles for the lower eccentricity orbits of the end-game phase. It was just not known until which point exactly the PTE could be reliable, therefore its performance had to be routinely monitored in order to identify early signs of degradation and if necessary react by increasing the margins, until this was possible. Dedicated results for this aspect are presented in a later section of this paper. Overall, although TGO behaved very well throughout the whole aerobraking, it required continuous attention from all teams, due to the inherent complexity of aerobraking, the trouble-shooting and tuning aspects described above, and due to some design features complicating its operability which could in retrospect have been better streamlined (e.g. interactions among different functions, partially automated FDIR, and the sheer number of commands needed to guide the S/C through the aero-pass and exoatmospheric activities).

The second major limiting factor was identified in the ground prediction accuracy of the commanded pericentres. In fact, although TGO would shift all nominal commands based on PTE predictions, the same was not implemented for the execution times of the autonomous manoeuvres (both FRMs and SPMs), which were instead triggered via ground-commanded apocentre tables. While the rationale for this decision was reasonable, i.e. the concern that PTE failures could be propagated through a safe mode, this had huge consequences on operations. In retrospect, it would have for instance been better to allow ground to decide whether to propagate PTE information through the safe modes or not, or to implement a further on-board check as MRO's Navigation Performance Monitor [15]. In fact for TGO, pop-up manoeuvres being at a fixed time, the ground prediction errors of the apocentre times could never be allowed to become too large, to avoid the risk of executing a popup in a completely wrong direction. As a consequence, a PMON had to be added to check the deviation between PTE and ground prediction (DT_PTE) of the upcoming pass, which would itself trigger a safe mode due to large ground prediction error, even in the absence of any actual S/C anomaly. The threshold for such PMON was set to $1/8^{th}$ of the orbital period, which would still allow for a comfortable increase of pericentre height with an off-apocentre SPM. This meant that the ground prediction window needed to be adjusted across the aerobraking to ensure that such performance could be achieved, even in the presence of an extremely unpredictable atmospheric density. Figure 6 shows the result of the assessment of the expected ground navigation phase error for decreasing orbital periods, a-priori computed by assuming a 30% error on the Atmospheric Scale Factor (ASF), i.e. by simulating a constant bias with no noise for the atmosphere calibrations within the Orbit Determination (OD). The comparison with the DT_PTE threshold ($1/8^{th}$ Torb) led to the decision of performing FD cycles, better described in the next section, initially every 2 days (3.5 days of prediction horizon) and then every day (2 days prediction horizon) starting from about 5 hours of orbital period. Moreover, the aerobraking regime would be lowered by about 30% at the 6 hours mark [3], as visible in the discontinuities of Figure 6, to further reduce ground prediction errors. Finally, based on the same results, it was also decided to terminate the aerobraking when reaching an altitude of roughly 1000 km instead of the original target of 400 km, due to the high risks related to both PTE and ground prediction performances on near-circular orbits. Even with these precautions and frequent ground updates, there was no way to ensure in advance that no DT_PTE safe mode would be triggered, since Mars atmosphere is known to possibly present sharp increases at times. Therefore, continuous monitoring of the atmosphere calibration results and forecasts also became a critical part of the daily FD activities, with the aim of reducing the likelihood of spurious safe modes, which would result in very large propellant penalties. More details on the atmosphere modelling and dedicated results for the ground prediction errors are presented in later sections of the paper.

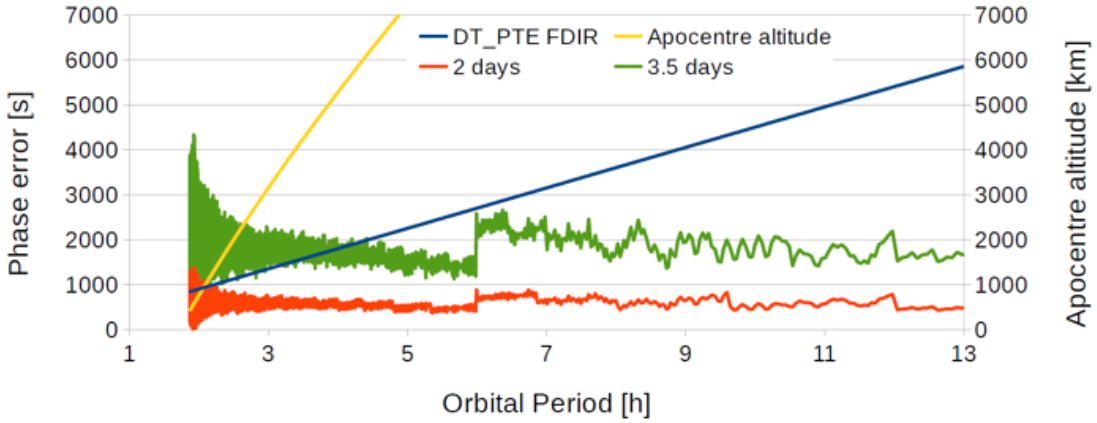

Figure 6: Expected ground prediction error of the orbital phase for 2.0 and 3.5 days prediction windows, assuming a constant over- or under-estimation of the atmospheric scale factor of 30% on each orbit.

III. Flight Dynamics Cycle Operations

The FD team at ESOC was in charge of TGO navigation and generation of all GNC commands guiding the S/C in its aerobraking. As mentioned in the previous section, this was carried out in short term "FD cycles", executed every 2 days in the bulk of the aerobraking and on a daily basis during the most critical phases: the walk-in of March 2017 and the end-game of December 2017-February 2018. For an overview of the aerobraking timeline and control corridor, as well as of the FD subsystems, see Ref. [3]. FD cycles for TGO aerobraking started at an a-priori defined Data Cut-Off (DCO) time with the processing of accelerometer, thruster, and events TM, to produce smoothed ΔV pulse files. At the same time, the S/C health was assessed from TM and a preliminary evaluation of the ASF of the latest aero-passes performed on the basis of accelerometer data. In parallel, radiometric tracking and meteorological data from ESTRACK and DSN stations was pre-processed, and then used in combination with the TM files as inputs for the OD process, to reconstruct the S/C orbit. Within the OD, additional uncertain parameters were estimated, of which the most critical was the ASF of the currently used atmospheric model. Based on recent history, predictions for the future ASF were then produced as inputs for the trajectory propagation, manoeuvre decision and – in case a PRM/PLM was inserted in the plan – for its optimization. Generation of the GNC commands, covering for example pericentre / apocentre tables, attitude guidance and options, SA/HGA articulations, WOL and OCMs, were then generated based on the optimized orbit. Finally, auxiliary FD "products" as for instance orbital / attitude events, orbit / attitude files, etc., were prepared for use by other operational entities as the FCT or external parties. At the end of the FD cycle, the commands were delivered to the FCT, who was in charge of the merging with other platform activities (if any) and uplink to the S/C. Coordination and smooth decision making in collaboration with all players (FD, FCT, Industry, Ground stations, etc.) was ensured through daily coordination briefings [3]. Moreover, NASA's JPL navigation team was not only very valuable for technical exchanges and cross-validation activities during aerobraking preparations, but also actively involved in the critical walk-in and end-game operations. Within the agreement of shadow navigation support, JPL and ESOC have been exchanging OD solutions on a daily basis, with JPL practically acting as a FD "night shift" for what concerns the atmosphere calibration and orbit reconstruction tasks.

More details on each of the steps described above, which are summarized in the timeline of Table 3, are provided in the rest of this section. Note that the table provides average durations for the activities, while there was significant margin on FD side (12 hours vs. run times of 6-7 hours) and FCT side, with two uplink opportunities with different ground stations scheduled between FD delivery and commands execution start on-board. Note also that DCO was initially set to 8.00 local time, but was later moved to 13.00 for the end-game phase since this would allow to reduce by a few hours the commanding horizon [3].

Start time	Duration	Activity description
DCO	0.5 h	Processing of S/C TM to produce accelerometer & thrusters ΔV file, plus events file
DCO	1.0 h	Pre-processing of radiometric tracking data from ESTRACK and DSN
DCO	2.5 h	Assessment of the S/C status, analysis of the aero-passes and ASF from TM
DCO + 1 h	1.5 h	Orbit Determination plus assessment and prediction of the ASF
DCO + 2.5h	-	Internal FD meeting with manoeuvre decision (and other decisions when needed)
DCO + 3 h	-	Coordination meeting with all involved teams (FCT, FD, Stations, Industry, Project)
DCO + 3 h	1.0 h	Manoeuvre optimization and short term / medium term orbits propagation
DCO + 4 h	3.0 h	Preparation of all aerobraking commands and auxiliary products, delivered to FCT
DCO + 12 h	-	Official deadline for the delivery of the FD commands and auxiliary products

Table 3: Typical FD Cycle timeline of activities. Each activity includes complete Test&Validation (TV) checks

A. TM processing: S/C events timing, thruster on-times, accelerometer profiles

As most interplanetary S/C, TGO uses radiometric data as measurements for the OD process. For aerobraking, this was complemented with TM information which had to be extracted and pre-processed from the raw packets dumped from the S/C. An ad-hoc PMON was set up to detect on-board lock when two-way link was established after each pericentre pass (for which communications were lost), triggering after 10 minutes a dump of the full mass memory storing all the TM from the pass. At DCO, FD would analyse the available data, with the aim of rapidly producing three main inputs for the OD: 1) an event log, containing the on-board times of GNC mode transition and transponder locks, as well as the history of the MTL shift occurrences, used to precisely match the S/C behaviour in accelerations modelling (e.g. WOL and OCM times); 2) a thruster pulses file, containing the ΔV impulses in inertial frame provided by the thrusters during AEBM passes, cumulated over TM sampling periods of 12 seconds, obtained from the on-times using a calibrated RCT force model and used to include RCT accelerations in the OD; and 3) an acceleration pulses file, containing the ΔV impulses in inertial frame from accelerometer measurements over OCMs and AEBM passes. This was produced starting from raw data recorded by the OBSW at the 10 Hz clock frequency, and fully

dumped to ground for the OCM and AEBM periods. The 10 Hz data were processed by removing the effect of angular rates (from gyro data) on the linear accelerations at the Inertial Measurement Unit (IMU) location, removing the accelerometer biases averaged before and after the aero-pass, and cumulating the data in inertial frame over 1s / 5s intervals for OCMs/AEBMs, which corresponds to filtering both measurement noise and high frequency atmospheric variations. The resulting ΔV file was used in different ways within the OD, as explained in the next subsection. As an example, Figure 7 and 8 show the measured acceleration along the X axis for the last aerobraking pass on the 20th of February 2018, with the smoothed profiles derived in this case from a Gaussian filter.

Together with the TM processing, an extensive set of checks was carried out in parallel to each FD cycle by analysing and processing in a semi-automatic fashion a large set of TMs, with reports presented at the internal FD briefings and, if needed, escalated to the full operations briefings. Some examples include the verification of TGO's sensors and actuators (e.g. STR tracking performances and blinding checks, Sun Sensors currents, RW loading vs. ground predictions), the monitoring of its autonomy functions (e.g. PTE, PUDE), and the assessment of AEBM and OCM performances such as propellant consumption, ΔV realization accuracy, attitude control bands, aerodynamic stability, etc. Finally, the 10 Hz accelerometer data were also used to perform an independent estimation of the ASF, as well as a pass-by-pass fit of an exponential density model to the filtered data points, with the twofold purpose of verifying the ASF values from the OD and of keeping the instantaneous atmosphere scale height monitored.

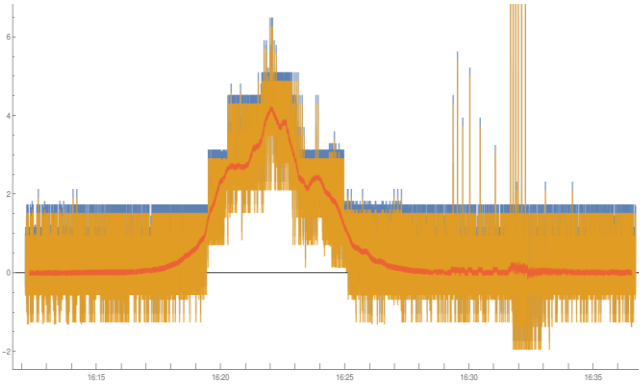

Figure 7: Example of 10Hz accelerometer data [mm/s^2] Orange: raw, Blue: unbiased, Red, filtered.

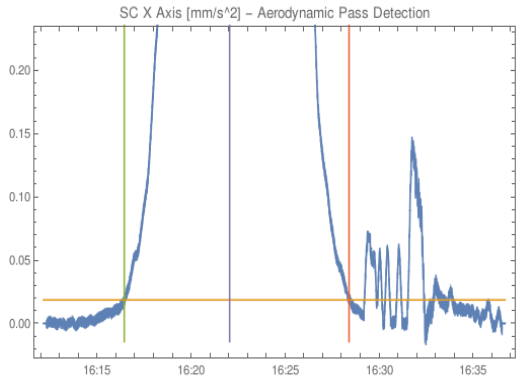

Figure 8: Zoom of the left graph on atmosphere threshold level (0.5 mPa, filtered acceleration only)

B. Orbit Determination:

TGO's OD is based on Doppler measurements in the two-way coherent X-band link between the spacecraft HGA and a large (30 to 70 meters) ESTRACK or DSN dish on Earth, with the line of sight information permitting a very accurate determination of the orbital period. After each atmospheric pass in aerobraking, the spacecraft slewed to Earth pointing and the two-way coherent link had to be re-established. In order for the on-board transponder to lock on the uplink signal frequency, an uplink frequency sweep was required. However, due to uncertainties in the orbital phase and aerobraking attitude, it could not be known in advance when the spacecraft would be re-acquired. Thus the strategy that was used to guarantee an earliest possible lock was to perform a permanent contiguous series of uplink sweeps (see examples in Ref. [3]). The sweep range was several tens of kilohertz while the rate was one kilohertz /s. For the purpose of modelling the Doppler observations in the orbit determination, it was required to know precisely the uplink frequency. Due to the sweep rate, small errors in uplink ramp timing could cause larger than usual modelling errors. This happened in various occasions with New Norcia's Intermediate Frequency & Modem System (IFMS) equipment, and it was necessary to calibrate the delay in the timings of the uplink frequency ramps.

Another issue encountered in some occasions with the aerobraking ODs was poor convergence. In fact, due to large prediction errors after several atmospheric passes, especially in the end-game, Doppler pre-fit residuals were usually large and could cause a divergence of the OD filter. To remedy this problem, the OD was often done in multiple stages, starting with a short observation arc and expanding it progressively when convergence was achieved for the current arc. Although this method required some manual iterations, it proved very effective in solving the experienced divergence issues.

Even though the above mentioned aspects as well as other OD configuration details are of some relevance, the modelling of the Mars atmosphere and of the resulting accelerations on the S/C constitute the most interesting aspect of aerobraking navigation. For TGO, atmosphere density (and sometimes wind) models were used to compute the drag acceleration using a flat plate model for the S/C, since the aerobraking attitude is not known a priori and feeding TM information for that purposes was not deemed worth the effort, nor sufficiently robust to TM outages. The only

free parameter in the atmospheric models is therefore the ASF, scaling the above drag model. This clearly cannot accommodate lift (in the S/C XY plane, perpendicular to the velocity, mostly due to non-zero aerodynamic stability angle), side-slip (out of plane component mainly due to attitude errors) and accelerations time-shift (delay between actual and modelled maximum density). To account for these effects, a set of four small impulsive and direction-constrained manoeuvres centred on pericentre times was solved-for in the OD. The manoeuvre time references were set to the pericentre times for a preliminary orbit determination or they were adjusted to match the actual pericentre times by a dedicated observation model, acting as a constraint within the OD.

In parallel to the orbit reconstruction performed using atmospheric density models, ODs using TM data from the accelerometer ΔV file were regularly run since the beginning of aerobraking for robustness, estimating a scaling factor on the data from the TM file, with the purpose of validating the orbit solution obtained with the atmospheric model. To prepare for the end-game phase, ESOC FD also developed the capability to process and use integrated accelerometer measurements as a new observation type in its OD software. The use of these measurements was expected to be beneficial in those cases when radiometric data could not provide sufficient observability over the different scaling factors of consecutive aerodynamic passes. For TGO, this covered the cases when a PLM/PRM was scheduled at apocentre during the end-game, with no time to slew to Earth pointing and therefore no Doppler data for the whole exoatmospheric arc, or any S/C or ground station contingency resulting in the loss of radiometric data between two – or more – aerodynamic passes. The use of integrated measurements instead of direct acceleration data is justified by better stability and convergence properties, with two possible observation types: the integral of non-gravitational acceleration magnitude over an aerodynamic pass, or the integral of the Cartesian components of in an inertial frame over the pass. A similar approach available at NASA JPL was used in cross-validation tests by the two agencies, and is described in greater details by JPL in Ref. [16].

Operationally, the use of accelerometer data as measurements provided further confidence in the OD solutions, via regular pass-through (i.e. pre-fit residual check) as well as periodic parallel OD runs. Moreover, this proved to be very useful when an issue at New Norcia on the 30th of January (orbit period of 2h46min) resulted in the loss of a nearly complete Doppler station pass, covering 4 atmospheric passes. In this case, TM data was used for the operational OD providing an estimate for the ASF of the single passes, which would not have been otherwise available. This case was actually very similar to a test scenario during the development phase, where the loss of a Doppler pass corresponding to 4 pericentres had been simulated, which was showing a very good agreement between the OD solutions and ASFs with and without the Doppler pass, when using the accelerometer data as measurements.

C. Atmospheric modelling:

As described earlier in the paper, one of the limiting factors enabling continuation of the aerobraking until the target altitude was a sufficiently accurate ground prediction of the orbital phase for the upcoming pericentres within the commanding window, for which a sufficiently accurate forecast of the future average atmospheric density was needed. Moreover, the actual aerodynamic load for each future pass was constrained by the thermal and mechanical limits of the S/C (700 mPa, 2800 W/m^2, 500 kJ/m^2). Upon suggestion by JPL, a 150% margin with respect to these limits was taken [3] when designing the long term aerobraking corridor, as well as the short term pericentre control strategy (i.e. one of 280 mPa, 1120 W/m^2 or 200 kJ/m^2 was the active constraint in the trajectory optimization), but satisfaction of these limits was still not ensured. In fact, Mars upper atmospheric layers density is far from being predictable even with the most complex global circulation models, since we lack real-time in-situ observations which are needed to calibrate such models on a short-term basis. Aerobraking experience from previous JPL's missions [8-13] had shown that orbit-to-orbit variability around Mars can easily reach 100% (i.e. density doubled or halved in successive passes), resulting in the large suggested margins and making estimation of an average value on a short term basis challenging. Additionally, the average values largely drift due to long-term, planet-wide effects, and rapid build-up of atmospheric density - within a day or so - can be expected in case of a global dust storm onset. Although TGO's aerobraking was completed before the start of the dust storm season, predicted not earlier than March-April 2018, very large variations of the average ASF were observed throughout the year of aerobraking, due to global phenomena which can be qualitatively explained with atmospheric physics but cannot be quantitatively predicted. Pass-to-pass variability was also similar to previous missions, with noise in the order of 100%.

Atmospheric modelling was therefore key to the effectiveness of TGO FD planning cycles, both to minimize the likelihood of exceeding the design limits or of triggering expensive, spurious, safe modes due to DT_PTE violations. Three different models were implemented: a simple exponential model with a constant scale height, the European Mars Climate Database (MCD) in its version 5.2, using the "climatology average solar conditions scenario", and JPL's Mars Global Reference Atmospheric Model (MarsGRAM, 2010 version), configured as per JPL suggestions. For all models, an ASF per pass was estimated in the OD, and an average over 10 to 20 passes was computed to be used for predictions. In preparation of the end-game, a "wave model" was also implemented, superimposing a longitude

dependency on the exponential model by fitting the amplitudes and phases of the diurnal tides, up to wave number 3, as in Equation (1). This approach was already developed by JPL when observing strong longitude dependency in some atmospheric regions for MGS [8-9], although such dependency has been later observed to often break down [10-13] and to only provide marginal improvements in terms of phase prediction accuracy [12-13].

$$\rho = \rho_h^{EXP}(h; H_s, h_0, \rho_0) \cdot \overline{SF(t)} \cdot (1 + \eta(lon, t)) \quad \eta = A_0 + \sum_{k=1}^{3} A_k \cos(k \cdot lon + \varphi_k) \quad (1)$$

All the above models were routinely assessed off-line, including variations of the main configuration parameters, but a single model had to be selected as reference for operations. During the first walk-in, MCD was used for this purpose, but it was soon found not to provide any significant advantage in prediction capabilities with respect to the simple exponential model. Similar results were obtained with Mars-GRAM, hence it was decided after less than 2 months to switch to an exponential model with a 8-km scale height, of comparable prediction accuracy but simpler use and especially of much more direct interpretability. This was kept until few weeks into the second walk-in, when the scale height was reduced to 6 km due to observational evidence, also having contributed to triggering a FRM while descending in the atmosphere. During the end-game, the wave model was also actively checked on a daily basis and used to support manoeuvre decisions, but was never phased into the operational OD. See Ref. [3] for more details on the models operational timeline, while an overview of TGO atmospheric modelling results is given later.

D. Manoeuvre decision and trajectory optimization

With the OD solution approved by the TV team, TGO's FD cycle continued with a manoeuvre decision, reached in the internal FD briefing on the basis of the LTP trajectory [3] defining the target aerobraking regime. For most of the aerobraking, the target heat flux of 1120 W/m^2 was the active constraint. Below 6 hours orbital period this was reduced by 30% to improve ground predictions [3], with the heat load then becoming active in the last couple of weeks of the end-game. To support the decision process with quantitative results from a simple trajectory propagation and one or more PRM/PLM optimization runs, predictions for the SRP acceleration and, more importantly, for the ASF were fed from the OD process. These were provided in a prediction parameter file containing the atmospheric prognosis in terms of the applicable atmospheric model (e.g. exp. 6 km) and 5 different ASF values: average, minimum, maximum, minimum peak, and maximum peak. The average ASF was the only one used for propagation and optimization of the operational orbit, and generation of future commands. Minimum and maximum values were instead used for the validation of the commands for worst-case low or high average passes, and the peak values were considered for the operational margins with respect to S/C design limits.

PRM and PLM were inserted based on the latest predictions of the average ΔV of all future pericentres in the commanding window, to be kept as close as possible to the LTP profile, and of the peak heat flux among these pericentres, to be kept below the target for the current aerobraking regime. Note that these do not only depend on the ASFs provided by the OD, but also on the natural trend of the pericentre altitude, which can vary by several hundred meters per orbit due to the non-uniformity of Mars gravity field, and on longitude-dependent atmospheric effects, partially captured by the wave model. No rigorous rule for manoeuvre decision was set-up, but rather a combination of heuristic criteria was applied, such as: 1) during walk-in, reduce altitude in progressively smaller steps to properly characterize the atmosphere, with final steps of about 3 km height change; 2) include PRM if the active constraint is exceeded by more than e.g. 5%; 3) include PRM / PLM if the average ΔV is above / below the LTP target by more than e.g. 10%; 4) include PRM / PLM if necessary for collision avoidance reasons with other natural or artificial satellites, or even if it can help to improve conditions for future close approaches; 5) do not include a PRM / PLM manoeuvre if its optimized size would result in less than 0.5 km of pericentre altitude change; 6) when including a PRM / PLM, consider future altitude variations and possibly the predicted peaks from the wave model longitude dependency to decide when the manoeuvre should be executed. Overall, these rules resulted in the execution of 67 OCMs, of which 15 in the pre-conjunction part (10 walk-in PLMs, 1 walk-out PRM, 2+2 corridor PLMs/PRMs) and 52 in the post-conjunction part (6 walk-in PLMs, 1 walk-out PRM, 1 autonomous FRM, 17+27 corridor control PLMs/PRMs), for a total ΔV of about 51 m/s, to be compared with a total drag ΔV of about 1017 m/s [3].

Figure 9 and 10 show one of the most interesting phenomena encountered in the manoeuvre optimization tasks. As mentioned, gravity "kicks" from the planet at the pericentres typically result in hundreds of meters of change of altitude at the following pass. This usually averages out, with some passes increasing and some other decreasing the orbital period. However, when the orbit is in a resonance with Mars rotational period, the same longitudes are flown for several days in a row, which can result in a continuous increase or decrease of the pericentre altitude. Such trend is not predictable until a day in advance or so, since phase prediction errors result in different sets of longitudes being flown during the resonance, with potentially very different trends. The pericentre longitudes flown close to the 3:1 resonance are reported in Figure 9, while Figure 10 shows the predictions with average, minimum and maximum ASF

from 2 days before entering the resonance, which show a maximum difference of about 13 km in the altitude after the exit from the resonance. A-posteriori, the atmosphere was similar to the predicted average case, which resulted in daily PLMs of about 1km for 7 days over the resonance period, to keep the planned aerobraking regime.

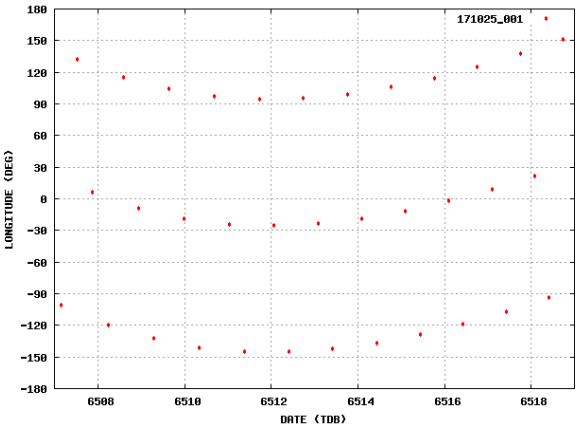

Figure 9: As-flown pericentre longitude evolution vs. MJD2000, 24/10 to 01/11 2017, 3:1 resonance.

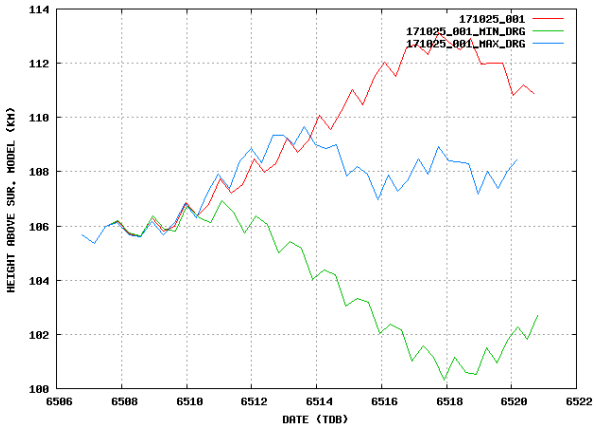

Figure 10: Predicted pericentre altitude evolution in the same 3:1 resonance period, different ASFs.

E. Generation of FD commands:

Based on the optimized trajectory, if necessary including one or more manoeuvres, the final step in the FD cycle was to generate all commands required to execute the nominal aerobraking activities and to cover the contingency scenarios for the near future. Typically few days of commands were produced and uplinked to the S/C, in order to allow for continued aerobraking operations in case of very serious ground issues resulting in failed uplink of the next cycle. For all ESA's S/C, FD is in charge of producing all GNC-related commands. In order to simplify and automate the process, this is done through a set of pre-defined command sequences owned by FD, so that only the time tag and the parameters which depend on each specific case have to be filled in at FD cycle level. For Exomars TGO, the same approach was followed, but for a much more complex system with respect to other interplanetary S/C, in particular due to the significantly larger number of activities and single commands. Nominal aerobraking operations required in fact about 120 commands per orbit, including guidance profiles (attitude, Sun, Earth, and STR velocity vector) based on Chebyshev polynomials with multiple segments, SA / HGA articulations, GNC mode and sub-mode transitions, accelerometer bias calibrations, WOLs, and a large set of PMON thresholds for ensuring safety in aerobraking, such as the DT_PTE trigger for safe mode or axial acceleration trigger for the FRMs. On top of that, additional 120 commands were needed for each OCM, and a series of pericentre and apocentre tables had to be included in each commanding cycle to allow for on-board shift of the MTL and for autonomous execution of FRMs and SPMs. To further complicate the commanding activities, dependencies among different nominal activities and interactions between nominal and contingency timelines had to be considered. To mention one of many examples, the guidance profiles around apocentre for orbits both with and without a planned OCM had be kept continuous with respect to the contingency guidance flown after FRMs. Finally, in order to avoid the need for a full mission planning run to merge FD commands with other FCT tasks, few additional command sequences related to platform activities were also taken over in the FD cycle. Overall, with a maximum of about 5000 commands stored in MTL, this meant that at most 42 orbits could be commanded at the same time, which allowed to cover less than 4 days in the end-game phase.

In preparation of the end-game phase, with the idea of minimizing the likelihood of a DT_PTE safe mode by further reducing the prediction horizon with respect to the 2 days allowed by the daily FD activities, an additional "Mini-cycle" step was added to the FD cycle timeline. According to this concept, successfully applied in the last 4 weeks, the on-board apocentre tables were quickly regenerated every day based on a simple orbit propagation after the OD, i.e. before the manoeuvre decision. Such updated tables could be uplinked to the S/C well in advance of the full commanding products, becoming active at 00.00 for a DCO at 12.00, rather than at 12.00 of the following day. By uplinking also consistent DT_PTE thresholds together with the updated tables, this allowed to reduce the prediction horizon from 2 to 1.5 days, with a very significant impact on the prediction accuracy, which grows quadratically with the number of elapsed aerodynamic passes. Due to the complexities described above, aerobraking commanding for TGO turned out to be the most time-consuming part of the FD cycle, but careful planning and execution together with rigorous checks by FD's TV team allowed to complete the aerobraking without major errors which could have endangered the safety of the S/C or at least its propellant budget.

IV.TGO Aerobraking Results

In this section, a selected set of results from TGO's aerobraking which are relevant to the previously described FD challenges and activities is presented. The overall performances in terms of aerobraking progress against LTP trajectories, total ΔV figures, atmosphere trends and both PTE and ground prediction accuracies, together with some examples of acceleration profiles, are already presented in Ref. [3]. Complementarily, Figures 11 to 14 report here the variations throughout the aerobraking of relevant parameters such as S/C pericentre altitude, peak heat flux, total and thruster ΔV, and the ratios of peak acceleration ASF over ΔV ASF and of aerodynamic ΔV over thruster ΔV. All graphs are split in two by the Solar conjunction wait-out period, with passes 1-125 executed in March-June 2017 and passes 126-952 in September 2017 – February 2018, as visible from the two walk-in phases at higher altitudes. In average, the peak heat flux was close to the target values of 1120 W/m^2 and then 780 W/m^2 after the 30% decrease, until around pass 700 when the heat load constraint started to be active. The gradual decrease between passes 300 and 350 of aerobraking regime is also clearly visible, as is the triggering of a FRM in pass 161 during the second walk-in. In that single occasion, the S/C design limits were slightly exceeded, peaking around 2900 W/m^2, although without damage on TGO. When comparing heat flux and ΔV profiles with the altitude profile, it is clear that very different density levels were encountered in different periods, for instance when decreasing density towards the Southern pole led the FD team to lower the pericentre from 110 km to below 104 km, between passes 400 and 600. The last graphs presents instead two important aspects. First, that when the target regime is reached, aerobraking becomes very efficient, with less than 1% of pass ΔV provided by the thrusters (orange curve). Second, that there is a significant variability in the ratio between scale factors reconstructed for the total integrated pass ΔV and the peak acceleration, which is proportional to the variability in scale height and has a direct operational relevance. Note that the vertical lines correspond to changes in the atmospheric model, from MCD to EXP–8km and then EXP-6km.

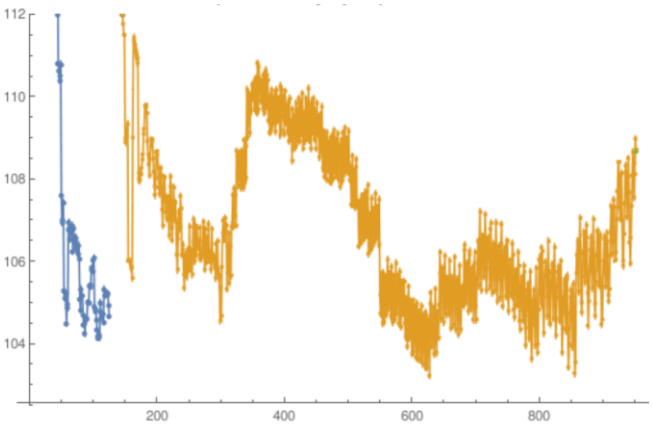

Figure 11: Pericentre altitude [km] above Mars ellipsoid vs. number of passes, pre/post conjunction.

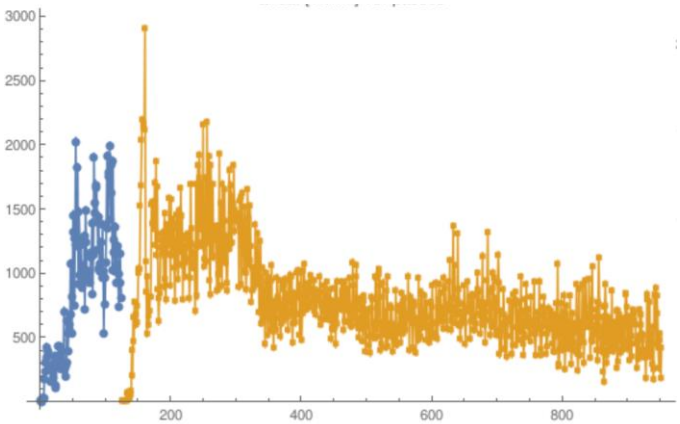

Figure 12: Peak heat flux [w/m^2] vs. number of passes, pre/post solar conjunction.

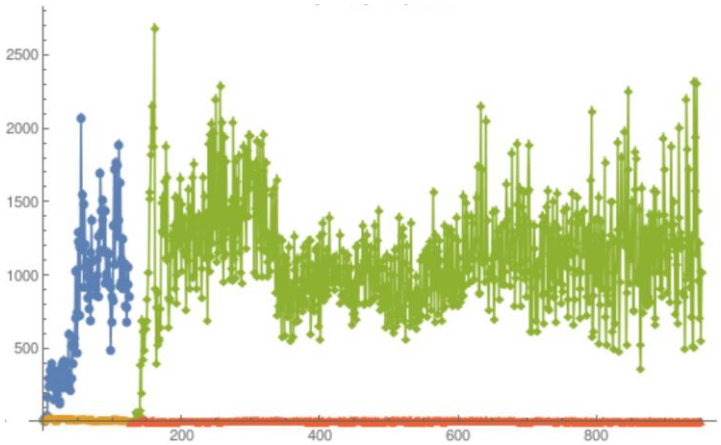

Figure 13: Total (blue/green) and RCT-only (orange/red) pass ΔV [mm/s] vs. number of passes, pre/post conjunction.

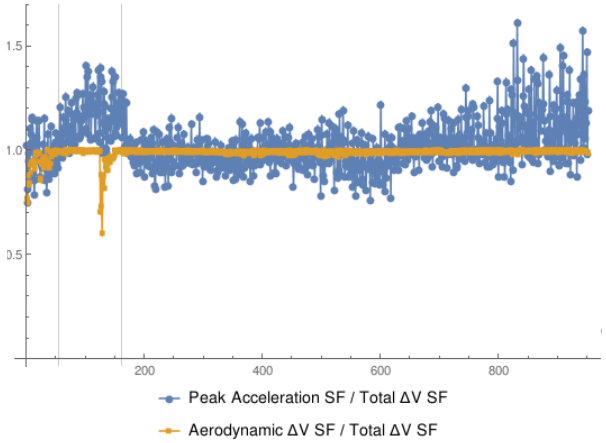

Figure 14: $ASF_{PeakAccel}$ / $ASF_{TotalΔV}$ (blue) and $ΔV_{drag}$ / $ΔV_{total}$ (orange) vs. number of passes.

A. TGO performance during AEBM passes

TGO's AEBM mode was designed to provide a robust mode for the atmospheric phases, based on aerodynamic stability for pitch and yaw control and thrusters for roll control. In order to avoid undesired pitch/yaw actuations during the pass, large control dead-bands in rate and off-pointing were implemented. These were tuned to 30 deg and 1.0 deg/s in pitch and yaw (S/C Y and Z axes) and 15 deg and 0.2 deg/s in roll (X axis). A typical rate and off-pointing profile for the whole AEBM period is shown for a sample pass in Figure 15, where the aerodynamically stable part is clear from the large, limited, oscillations around Y and Z axes, while the thruster actuations to control the X axis are visible in the high frequency rate oscillations from SA flexible modes excited by the actuations. Since the S/C was commanded into AEBM with zero rates to avoid loading the RWs, and a 4 minute margin was taken in the AEBM transition, an off-pointing of about 10 deg builds up before the atmosphere is reached, without any effect from the controller in the dead-band. Aerodynamic torques in the atmosphere then bring the S/C back to its target attitude. When the denser atmosphere is left, residual rates cause nearly linear increase of the off-pointing, until RD is entered and the thrusters bring the rates close to zero again for transition to the wheel controlled NOMR. Note that Figure 15 is only an example of possible behaviour. Often for instance, pitch/yaw actuations started before transition to RD when the 30 deg dead-band was reached, in presence of larger residual rates when leaving the atmosphere.

Overall, the required AEBM performances were fully met by TGO in flight, with peak AEBM rates well within the 2 deg/s FDIR limit, an average propellant consumption per pass slightly below the budgeted 10 grams/pass, and residual rates at NOMR entry loading less than 1 Nms on each wheel. However, the actual aerodynamic stability angle on the XY plane as derived from the processing of the measured angular rates, was found to be off from the 172.5 deg (7.5 deg from –X to +Y) in the aerodynamic database, which was being used for computing the guidance profiles. This is visible in Figure 16, where the off-pointing around Z is not oscillating around zero but rather around a positive angle of roughly 4 deg. In November 2017, it was therefore decided to change the stable angle to 168.8 deg, the average value from TM reconstructions. This led to immediate drop of the maximum Z rates (discontinuity around pass 390 in Figure 17), as well as to a (minor) reduction in the average propellant consumption per pass.

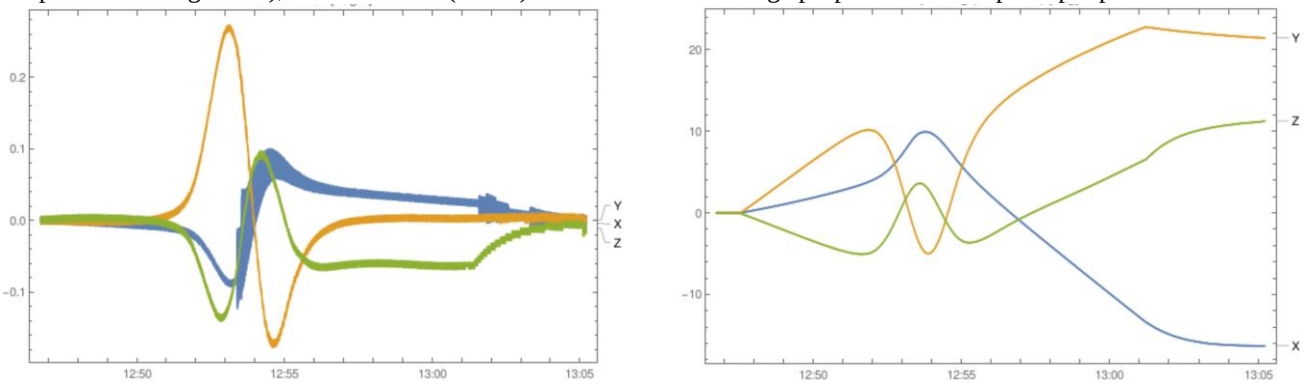

Figure 15: Measured rates (left, deg/s) and off-pointing (right, deg) around the S/C axes for a sample pass.

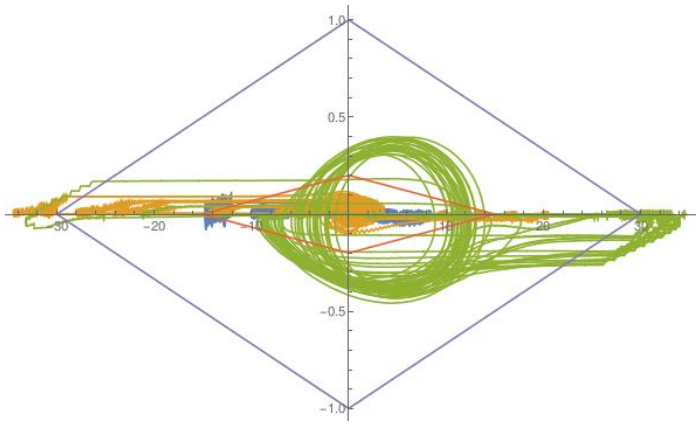

Figure 16: Rates [deg/s] vs. off-pointing [deg] around each S/C axis for 22 consecutive passes in mid-October.

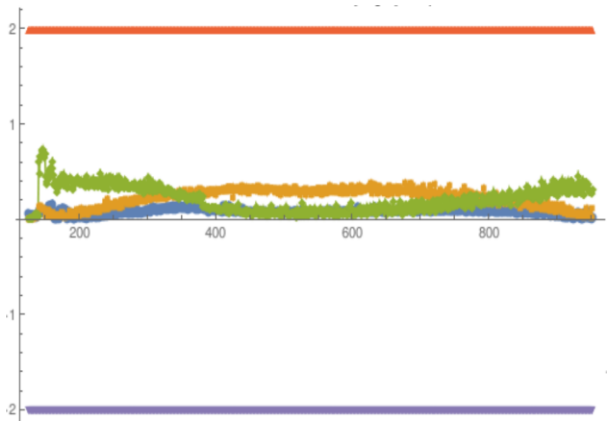

Figure 17: Max pass rate [deg/s] per axis (blue: X, orange: Y, green: Z) vs. number of passes.

To provide further insight, Figure 18 shows the accelerations along the three S/C axes for a typical aero-pass, which roughly correspond to drag, lift and side-slip components estimated in the OD. For each axis, the measured filtered acceleration (green) is compared with two different fits of an exponential model density where both scale height and scale factor are the fit parameters. In the first (blue), the angle-of-attack, side-slip angle and aerodynamic velocity needed to model the aerodynamic forces are computed by assuming the atmosphere is inertially fixed, while in the second (orange) by assuming it is co-rotating with Mars, with the actual conditions somewhere in between. The aero-pass shown in the example is rather regular in acceleration profile, building up to 865 mm/s and best fitted with a scale height of 6.5 km. Note that the short term oscillations in the drag result from actual atmosphere variations, not from off-pointing errors which only minimally affect the frontal area of the S/C.

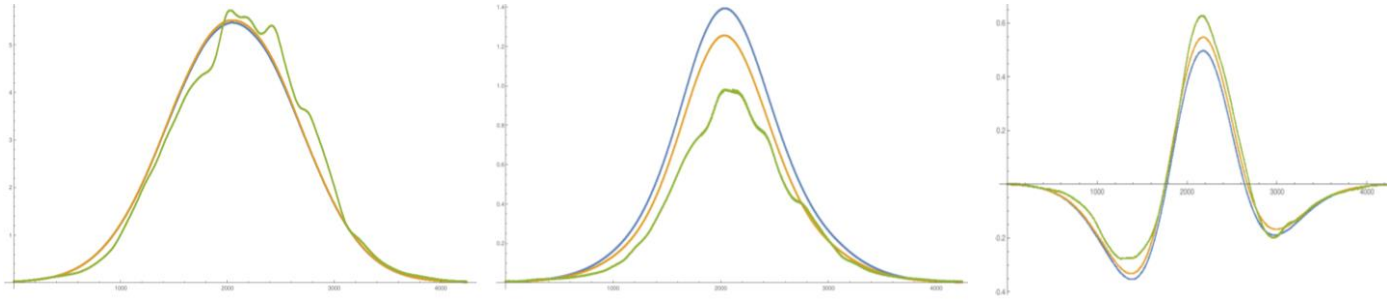

Figure 18: Example of acceleration profiles [mm/s^2] along X, Y, Z axes: measured (green) vs. atmospheric fits obtained using Mars-fixed atmospheric velocity (blue) and co-rotational atmospheric velocity.

B. PTE and ground prediction accuracy

As mentioned earlier, the two largest concerns of the FD team in terms of capability of reaching the target 1000 km apocentre altitude were the degradation of the PTE accuracy beyond the point which could be compensated with margins, and the worsening of the ground prediction of the orbital phase, possibly leading to a DT_PTE safe mode. It's also worth mentioning in this context that, after a safe mode in the last 10-15 days of the end-game, aerobraking would likely not have been restarted, since a direct OCM to the final altitude would have been comparable in propellant consumption. With respect to PTE accuracy, it was clear already after the initial walk-in that the performance in elliptical orbits was significantly better than the 240 seconds specification. With the exception of the last few weeks of aerobraking, the PTE accuracy was consistently better than 30 s in estimation of the past pericentre times and better than 60 s in prediction of the upcoming one. Moreover, the PTE started to be reliable already with dynamic pressures just above 10 mPa. Therefore, while for the first walk-in the MTL shift by the PTE was only enabled after about 3 weeks of monitoring, this was activated as soon as possible for the second walk-in after conjunction, in order to avoid having to include huge margins on the AEBM period. Starting from the end of January, the PTE accuracy in both estimation and prediction started degrading, due to growing irregularity and longer duration of the aerodynamic passes. Ref. [3] quantitatively shows the degradation in difference between PTE-estimated/-predicted and OD-reconstructed pericentre times, together with examples of the most irregular acceleration profiles. Nevertheless, PTE estimation and prediction errors never exceeded 90 and 150 s, still well within the specified 240 s and hence within the taken margins.

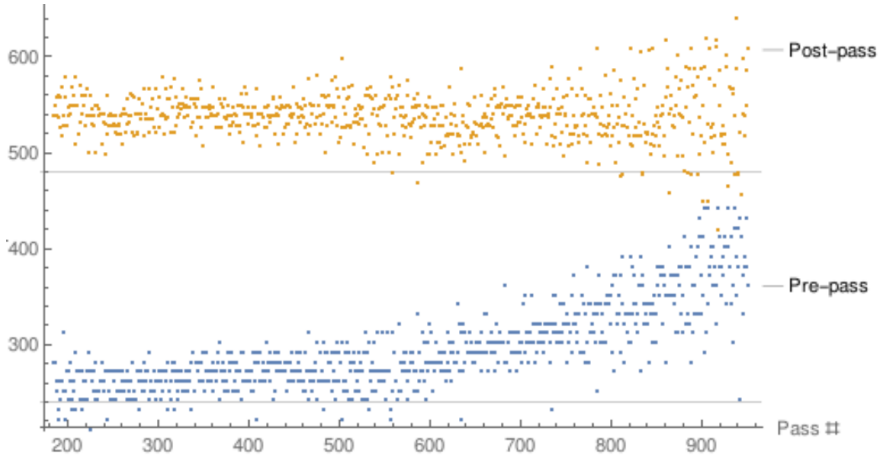

Figure 19: Margin [s] between AEBM entry/exit and start/end of the actual aero-pass, i.e. Qdyn>5 mPa.

Moreover, an additional margin had been built in the FD cycle strategy: when predicting the duration of the atmospheric passes (on the basis of the optimized orbit) in preparation of the commands generation, a threshold of 0.5 mPa was assumed to distinguish between atmospheric and exoatmospheric arcs. Since TGO was designed to cope with up to 5 mPa on RW, this gave an extra time margin with respect to the 240 s before and after each pass. More importantly, this extra-margin started to increase towards the end-game due to the lower orbital eccentricity (i.e. longer time spent between 0.5 and 5.0 mPa), balancing the increased PTE prediction errors. For this reason, the a-posteriori reconstructed difference between entering/exiting AEBM and reaching the 5 mPa threshold increased in average towards the end-game, as shown in Figure 19. Note however that the noise on the residual margins, both before and after the pass, increased significantly due to the degradation of the PTE for low accelerations.

With regards to the accuracy of orbital phase ground predictions, this could be directly monitored on ground through the DT_PTE TM parameter, i.e. the difference between ground-predicted and PTE predicted pericentre time. This was also monitored on-board to trigger a safe mode if exceeding the ground-commanded 1/8th of the orbital period. Figure 20 shows the full DT_PTE history for all 952 passes on the left, and a zoom for the last ~100 passes on the right, in comparison with the varying thresholds. The DT_PTE was updated on-board both at the exit of each AEBM pass, when the on-board prediction for the next pass was computed, and at the triggering of MTL re-population with a new set of FD commands, when the ground predictions for all future passes were refreshed. From the graphs, it's clear that the risk of triggering a DT_PTE safe mode was never too close, even though in several occasions about half of the FDIR level was reached. The largest absolute value was -2447 seconds just after the triggering of the FRM during the second walk-in. Both phenomena can be explained by a large under-estimation on ground of the ASF after the last two PLMs of the walk-in, due to a much lower scale height than the assumed 8 km as well as to a certain stiffness in the method of prediction of the future ASF, for which multiple passes have to be observed with a given trend before significantly affecting the average ASF value used for propagation. On the right side zoom, the FDIR limits start showing variations on top of the orbital period decrease, due to the introduction of the already described "Mini-cycle" concept. Note how the FDIR limits were adjusted to reflect the latest knowledge on the orbital phase, successfully ensuring an additional margin against DT_PTE safe mode.

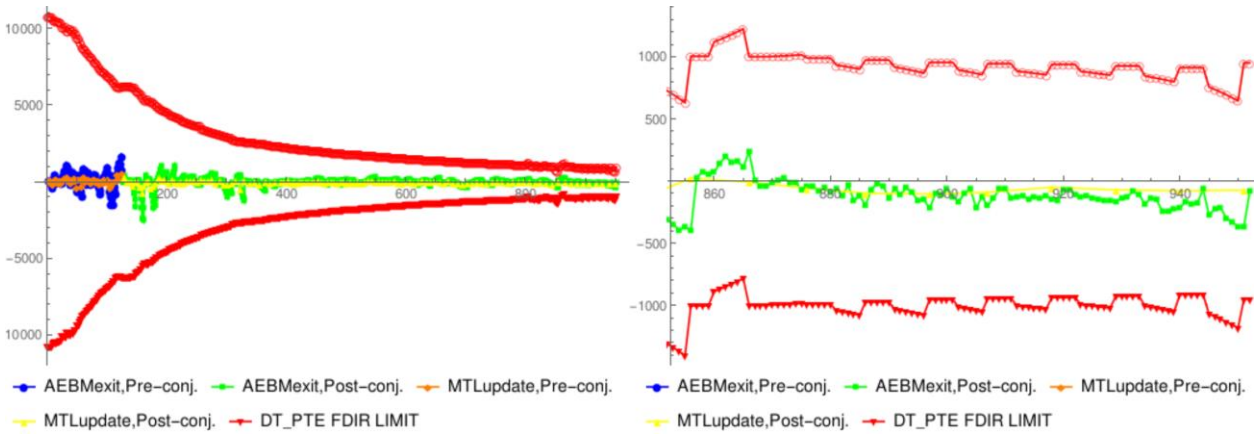

Figure 20: DT_PTE values [s] at AEBM exit and MTL update vs. pass number (right: zoom of the last 100)

C. Atmosphere modelling

TGO aerobraking provided a huge wealth of atmospheric data, having sampled the upper layers of the Martian atmosphere with its high accuracy accelerometers in the Southern hemisphere winter, from -10˚ to -73.6˚ latitude, covering 24 hours in Local Solar Time (LST) and with a Sun Zenith Angle (SZA) always above 90 deg, i.e. with pericentres always occurring in the night. These data confirmed the most operationally important aspects that were encountered by JPL with MGS, ODY and MRO, in particular the large short term variability of the atmospheric density as well as its global trends. Figure 21 reports the pass-to-pass variation of the ASF, i.e. the ratio of the scale factors of two successive passes, vs. the pericentre latitude, and its running standard deviation over 30 passes. The black curve corresponds to the initial part of the aerobraking, with TGO pericentres descending South towards the pole, and the red one to the final part, returning North after having reached the minimum latitude. The overall mean of the pass-to-pass variation is 1.05, with a standard deviation of 0.35 which is consistent with those measured by MGS (0.39), ODY (0.47) and MRO (0.36). Similarly, Figure 22 reports a "15-pass variability", computed as the ratio of a scale factor of a given pass divided by the average in the previous 15 passes, and its running standard deviation. As expected, the overall standard deviation decreases to 0.24, with a mean at 1.00.

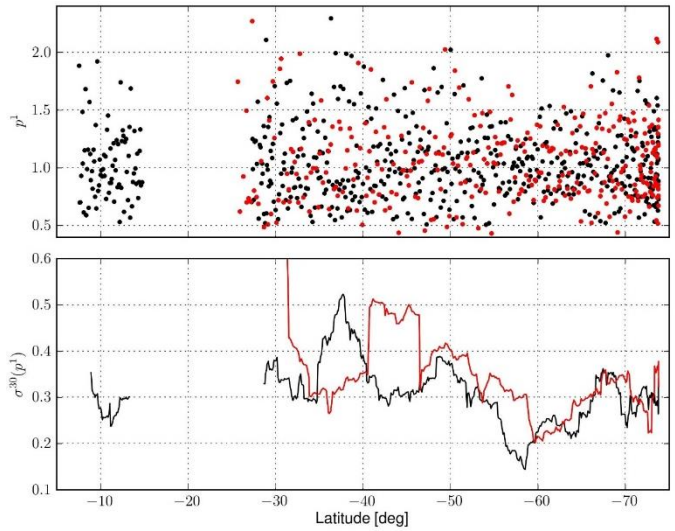

Figure 21: Pass-to-pass variability p^1 of the ASF (top) and its running standard deviation $\sigma(p^1)$ (bottom) vs. pericentre latitude. Black/Red: moving South/North.

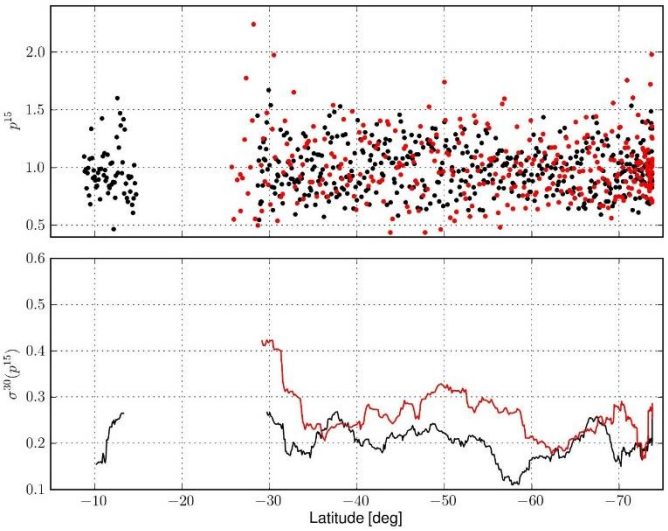

Figure 22: 15-pass variability p^{15} of the ASF (top) and its running standard deviation $\sigma(p^{15})$ (bottom) vs. pericentre latitude. Black/Red: moving South/North.

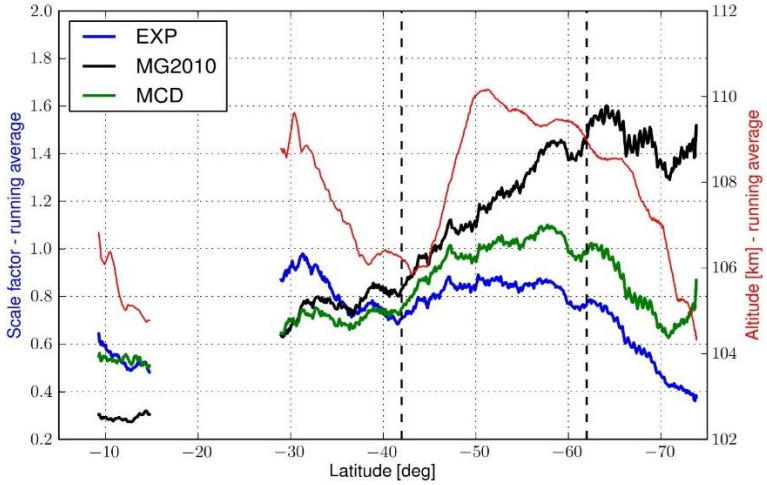

Figure 23: Running average of the reconstructed ASF vs. pericentre latitude for three atmospheric models.

Together with the pericentre altitude, Figure 23 presents instead the running average over 15 passes of the ASF vs. the South-bound latitude, for three representative models: MCD v5.2, MarsGRAM-2010 and exponential. The latter of course directly follows the actual atmospheric density, which remained approximately constant until -60˚ latitude. However, both MarsGRAM and MCD anticipated the density gradually decreasing between -40˚ and -60˚, which led to the continuous increase of the ASF. The density dropped sharply south of -60˚ once the aerobraking passes took place within the polar circulation zone. MCD and MarsGRAM predicted the existence of such a transition with an even stronger decreasing trend, but expected its onset at about -70˚ hence the initially decreasing then increasing ASFs in the polar region. These and other similar considerations indicate that complex models such as MarsGRAM and MCD provide qualitatively good descriptions of the main atmospheric phenomena. However, due to the lack of real-time observational data around Mars, these models cannot provide the exact transition points for such phenomena (think for example of predicting the exact location of the meandering jet stream on Earth without observations), often resulting in quantitatively wrong predictions in the short term. For instance, the longitude dependence is hard-coded in MCD even though this is a time-varying phenomenon well described by periodic fits of the wave model described earlier. As a consequence, complex models such as MarsGRAM and MCD do not bring any added value for short term aerobraking operations, as experienced for TGO in flight, leading to the decision of switching to the more straightforward and easy to interpret exponential model. However, these models can provide valuable insights for mission analysis, as they capture qualitatively well general trends and transitions to be expected. Note also that experience in the end-game phase showed that the wave model can provide non negligible reductions

of the RMS of the ΔV error, with about 15-20% improvement in average. This however does not necessarily translate into better DT_PTE values, due to the large effect that small errors in longitudinal location of the wave peaks can have on orbital phase errors. Since the improvement from the wave model was marginal, it was never used for official predictions, but it was qualitatively used in several occasions to support manoeuvre decisions.

V. Conclusions and lessons learnt

By providing a more detailed analysis focused on Flight Dynamics aspects, the work presented here complements a companion paper [3], which gives a higher level overview - covering all involved players - of TGO's successful aerobraking operations. From a FD perspective, TGO aerobraking presented several difficult challenges, which could be met thanks to a large effort in the preparation, analysis and validation of the operational approach, as well as in the actual execution of critical operations, with extended working hours for a prolonged period of time.

Due to TGO's ballistic coefficient and thermal constraints, aerobraking from 24 to 2 hour orbital period required longer than with previous JPL's S/C, with 10 months of atmospheric passes spit in two phases by a solar conjunction. Throughout this period, the FD team has been continuously executing a complex series of activities, grouped under the term of FD cycle, consisting of TM processing, Orbit Determination, Manoeuvre decision and optimization, and generation of the GNC commands, which are all described in more details in the paper. A FD cycle nominally required about 7 hours of work for a team of 10 people, without considering possible processing issues, and was executed every 2 days for the bulk of the aerobraking, increasing to daily frequency in the most critical phases: the first month of walk-in and the last two months of end-game. Moreover, extensive preparations were needed over a period of more than 2 years, and intense trouble-shooting at the beginning of aerobraking also required significant off-line analyses. The most critical aspects contributing to the high workload were the tight S/C schedule for short orbits, mainly due to the low RW slewing rates, the lengthy set-up and tuning of the extensive on-board autonomy and FDIR functions, and the very complex commanding strategy for aerobraking.

However, thanks to the careful analysis, continuous tuning and refinement, and thorough validation of the operational approach, as well as to a steep learning curve and quick response to minor anomalies during the initial walk-in, aerobraking operations progressed extremely smoothly. The target apocentre altitude of 1000 km was reached almost one month ahead of schedule, without ever triggering a safe mode and with a significant propellant saving. The extensive preparations, absence of major operational mistakes and a very good performance of TGO made such an achievement possible.

Relevant results are presented in the paper for the overall aerobraking progress, the S/C behaviour in the AEBM passes, the performances of on-board autonomy functions and ground navigation team, and the difficult modelling of the unpredictable Martian atmosphere. Two limiting factors were identified as major concerns from a FD perspective for the successful termination of aerobraking, namely the prediction accuracies of the on-board PTE function and of the ground navigation team, expected to degrade in the challenging end-game phase. Both were appropriately tackled, as detailed in the paper, by introducing sufficient margins against PTE errors and by minimizing the ground prediction horizon through daily FD cycles and the Mini-cycle concept. Nevertheless, although it may seem from these results that reaching lower apocentre altitudes through aerobraking rather than propulsive manoeuvres could have been attempted, it is the opinion of the FD team that this could only have been done at significant risk for the S/C.

Overall, ExoMars TGO aerobraking was a success for all teams involved, and largely increased ESA's experience in this scenario. From a FD point of view, several key lessons can learnt from this, which may be beneficial for future aerobraking missions at Mars. First, in order to improve the drag efficiency and therefore reduce the required man-power, an aerobraking S/C should ideally have a much lower ballistic coefficient and higher thermal limits, with JPL's latest MRO mission as an example. Moreover, it should aim at a better agility, allowing for more margins in the orbital timeline, and at a more streamlined commanding approach and autonomy/FDIR functionalities, which would result in simpler preparation and execution of the aerobraking operations. Finally, the PTE information should be propagated through safe modes, either implementing an on-board logic to validate its performances or by deferring to ground the choice of enabling the propagation. This would in fact allow to time-shift the autonomous pop-up OCMs, drastically reducing the required ground prediction accuracy, extending the feasible commanding horizon and therefore alleviating the need for very frequent FD cycles.

Acknowledgments

The authors would like to acknowledge all colleagues in the FD team for interplanetary missions, as well as the FCT and all other ESA support teams, who contributed to the success of TGO's aerobraking campaign. Special thanks to Robert Guilanya, Alfonso Rivero and David Jesch, who provided inputs for this paper, as well as to TAS Industrial team, who provided valuable support and knowledge of TGO systems, within a smooth and fruitful collaboration.

References

[1] Svedhem, H., and O'Flaherty, K., "Exomars 2016 Mission, Brief Description of TGO and Schiaparelli," *ESA public report*, 2016.

[2] Yamaguchi, T., and Kahn, M., "Mission Design and Navigation Analysis of the ESA Exomars Program," *24th International Symposium on Space Flight Dynamics (ISSFD)*, Laurel, Maryland, USA, May 2014.

[3] Denis, M., et al., "Thousand Times Through the Atmosphere of Mars: Aerobraking the ExoMars Trace Gas Orbiter," *SpaceOps 2018*, Marseille, France, May 2018.

[4] Guilanya, R., and Companys, V., "Operational Approach for the Exomars Aerobraking," *23rd International Symposium on Space Flight Dynamics (ISSFD)*, Pasadena, California, USA, November 2012.

[5] Cassi, C., et al., "The ExoMars 2016 Mission Flight Performances until Achievement of the 1-sol Orbit," *68th International Astronautical Congress (IAC)*, Adelaide, Australia, September 2017.

[6] Renault, H., et al., "GNC Design and In-Flight GNC Behaviour," *GNC 2017*, Salzburg, Austria, June 2017.

[7] Giorgini, J., et al., "Magellan Aerobrake Navigation," *British Interplanetary Society, Journal*, vol. 48, no. 3, March 1995.

[8] Johnston, M.D., et al., "The Strategy for the Second Phase of Aerobraking Mars Global Surveyor," *AAS 99-303*, 1999.

[9] Esposito, P., et al., "Navigating Mars Global Surveyor Through The Martian Atmosphere: Aerobraking 2," *AAS 99-443*, AAS/AIAA Astrodynamics Specialist Conference, 1999.

[10] Smith, J.C., and Bell, J.L., "2001 Mars Odyssey Aerobraking," *Journal of Spacecraft and Rockets*, Vol. 42, No. 3, May-June 2005.

[11] Mase, R.A., Antreasian, P.G., Bell, J.L., Martin-Mur, T.J., and Smith J.C., "The Mars Odyssey Navigation Experience," *AIAA 2002-4530*, AIAA/AAS Astrodynamics Specialist Conference and Exhibit, 2002.

[12] You, T.H., et al., "Navigating Mars Reconnaissance Orbiter: Launch Through Primary Science Orbit," *AIAA 2008-6093*, AIAA SPACE 2007 Conference & Exposition, 2007.

[13] Long, S.M., et al., "Mars Reconnaissance Orbiter Aerobraking Navigation Operation," *AIAA 2008-3349*, SpaceOps 2008.

[14] Damiani, S., Garcia, J.M., Guilanya, R., Munoz, P., and Muller, M., "Flight Dynamics Operations for Venus Express Aerobraking Campaign: a Successful End of Life Experiment", *25th International Symposium on Space Flight Dynamics ISSFD*, Munich, 2015.

[15] Kenworthy, J., Seale, E.H., and Dates, J.A., "Autonomous Fault Protection Orbit Domain Modeling in Aerobraking", *2007 IEEE Aerospace Conference*, USA, 2007.

[16] Young, B., "Practical Orbit Determination For Aerobraking With Accumulated Accelerometer Data," *Junkins Dynamical Systems Symposium*, 2018.